

OCEAN CARBON PUMPS: ANALYSIS OF RELATIVE STRENGTHS
AND EFFICIENCIES IN OCEAN-DRIVEN ATMOSPHERIC CO₂ CHANGES

Tyler Volk and Martin I. Hoffert

Department of Applied Science, New York University
New York, New York 10003

Abstract. An ocean carbon pump is defined as a process that depletes the ocean surface of ECO_2 relative to the deep-water ECO_2 . Three pumps are recognized: a carbonate pump, a soft-tissue pump, and a solubility pump. The first two result from the biological flux of organic and CaCO_3 detritus from the ocean's surface. The third results from the increased CO_2 solubility in downwelling cold water and is demonstrated by a one-dimensional upwelling-diffusion model of an abiotic ocean. In the soft-tissue and solubility pumps, working strengths are defined in terms of the ΔECO_2 each creates between surface and deep-water. Efficiencies of each pump are quantified as a ratio of working strength to potential maximum strength. Using alkalinity, nitrate, and ECO_2 to remove the carbonate pump signal from ocean or model data, the individual working strengths of the soft-tissue and solubility pumps can be calculated by scaling the soft-tissue's ΔECO_2 to the surface-to-deep ΔPO_4 . This technique is applied to a three-box ocean model known to demonstrate high-latitude control of atmospheric CO_2 through a variety of circulation and biological changes. Considering each pump separately reveals that the various changes which lower $p\text{CO}_{2\text{atm}}$ in the model are caused primarily by an increased solubility pump. Analysis of global ocean data indicates a positive solubility pump signal, subject to uncertainties in the C:P Redfield ratio and in the preindustrial $p\text{CO}_{2\text{atm}}$. If C:P = 105 and $p\text{CO}_{2\text{atm}} = 270 \mu\text{atm}$, the efficiency of the solubility pump is about 0.5. We suggest that this type of analysis of relative carbon pump strengths will be an effective method for inter-model and intra-model comparison and diagnosis of underlying oceanic mechanisms for $p\text{CO}_{2\text{atm}}$ changes.

Introduction

Models that simulate the steady-state distribution of total carbon dioxide (ECO_2) and various other tracers, such as carbon 14, temperature (T), phosphate (PO_4), nitrate (NO_3), oxygen (O_2), salinity (S), in the ocean can potentially be utilized for studying the variation of atmospheric CO_2 ($p\text{CO}_{2\text{atm}}$)

with ocean changes. A hierarchy of such models exists, consisting of simple box models [Keeling and Bolin, 1968], multi-box models [Bolin et al., 1983], one-dimensional models [Hoffert et al. 1981], two-dimensional models [Baes and Killough, 1985], and three-dimensional models [Maier-Reimer, 1984].

Employing primarily the simpler models in quantifying the relationship between ocean changes and $p\text{CO}_{2\text{atm}}$ is a relatively recent interest fueled by the discovery of lowered $p\text{CO}_{2\text{atm}}$ during the last glacial period [Neftel et al., 1982; Oeschger and Stauffer, 1985]. In general, $p\text{CO}_{2\text{atm}}$ is a function of the state of the ocean's surface properties, specifically, ECO_2 , alkalinity (TA), T, S, PO_4 , and silicate (SI) (see the appendix). Changes in natural $p\text{CO}_{2\text{atm}}$ in time scales in which it is in equilibrium with the ocean must correlate with changes in what is a rather complex distribution of these properties.

There are two general types of changes that the ocean's surface properties can undergo. One is a change in the total ocean-atmosphere inventory of a property. An example is the higher salt/water ratio during glacial times in which the assumption might be that the change in the average equals the change in the surface. The second type of change is where the total inventory remains constant, but the distribution of a property changes. An example here would be a change in the C:P Redfield ratio of organic detritus. Hybrids are also possible, such as a change in the PO_4 inventory that alters the vertical distribution of ECO_2 . Broecker [1981] explored these possibilities in developing the phosphate-extraction hypothesis for the glacial-interglacial $p\text{CO}_{2\text{atm}}$ levels.

Recent work in the direction of the second type is of interest because it examines changes in the processes within the ocean. For example, Broecker and Takahashi [1984] discussed changes in ocean circulation upon $p\text{CO}_{2\text{atm}}$, explored with a two-box ocean model put into two end-states, that of Redfield-ocean and a thermodynamic ocean. There is also the important group of three-box models which look at the role of various circulation magnitudes and high-latitude biology, temperature, and other

properties on pCO_{2atm} [Siegenthaler and Wenk, 1984; Knox and McElroy, 1984; Sarmiento and Toggweiler, 1984; Wenk and Siegenthaler this volume; Toggweiler and Sarmiento, this volume; Ennever and McElroy, this volume].

A problem with these models that change the distribution of CO_2 within a constant ocean-atmosphere inventory is that although they represent the global ocean in an exceedingly simple manner, they are fairly complex systems. Combining a simple marine biosphere with a simple circulation scheme and carbonate chemistry results in a model requiring a computer for experimentation. Understanding reasons for different states of a model is difficult enough, and comparing effects across various models is more so; we can reasonably expect this difficulty to magnify as models further up the hierarchy are employed for such studies.

The goal of this paper is to develop a quantitative vocabulary enabling us to compare different models. A key question is: can the numerous and potentially infinite model property variations that cause pCO_{2atm} changes be reduced to a smaller and finite set of more fundamental causes? One answer lies in the definition of what will be termed carbon pumps. Our approach will be to describe the pumps and formalize expressions for their relative working strengths and efficiencies. Applying these strengths and efficiencies will be shown to be valuable in analyzing both outputs of models and ocean data.

Carbon Pump Types, Efficiencies and Strengths

Although the term "pump" is most commonly associated with mechanical devices that create a pressure gradient, it also applies to processes that create or maintain a concentration gradient, such as the sodium ion pump in the membrane of a cell. The second sense is appropriate for the ocean carbon system. One of the distinctive features of ECO_2 in the world ocean is that the deep-water ECO_2 (ECO_{2d} as global mean) is higher than the surface mixed layer ECO_2 (ECO_{2m} as global mean). This is true of all ocean regions, with the global means of $ECO_{2m} = 2012 \mu\text{mol/kg}$ compared to ECO_{2d} (below 1200 m) = $2284 \mu\text{mol/kg}$ [Takahashi et al., 1981a]. What maintains this vertical carbon gradient? Since diffusive ocean mixing is always actively destroying differences in concentration, there must be a continuously counteracting process that is maintaining the vertical carbon gradient. The active process might be termed a global ocean carbon pump; its action is important because of the sensitivity of pCO_{2atm} to ECO_{2m} .

The global ocean carbon pump is actually a system of components, each of which is a pump itself. Three such components may be distinguished.

Two of the pumps are biological, and will be termed the soft-tissue pump and the carbonate

pump. They are due to the action of organisms at the ocean's surface removing ECO_2 and incorporating it into organic and calcium carbonate particles, respectively. These particles are transported into the depths through gravitational settling and active biotransport [Redfield et al., 1963] where the carbon and other components are returned to their dissolved, inorganic forms.

The important effect of the soft-tissue pump on the vertical distribution of ECO_2 , PO_4 , NO_3 , and O_2 is well recognized [Broecker, 1983]. PO_4 and NO_3 affect TA; the surface depletion of PO_4 and NO_3 by the soft-tissue pump raises TA relative to what it would be otherwise. The reduction of ECO_2 and elevation of TA by the soft-tissue pump both serve to lower pCO_{2atm} in equilibrium with the surface at a constant temperature and salinity.

The carbonate pump has competing effects on pCO_2 : the lowering of TA due to the removal of calcium ions raises pCO_2 , while the lowering of ECO_2 through the carbonate ion removal lowers pCO_2 . The TA effect is dominant in the vicinity of present surface conditions, and so a stronger carbonate pump raises pCO_2 . A full treatment of the carbonate pump in the terminology of strength and efficiency, as will be done for the soft-tissue pump, must be deferred to a later work. The primary concern here will be to remove the carbonate pump signal from the ECO_2 data.

The third pump refers to a process which we term the solubility pump and is driven by the CO_2 solubility differences of warm and cold water, i.e., the surface and deep-water. The solubility pump can be examined through a modeling experiment.

We use the one-dimensional upwelling diffusion ocean model of Hoffert et al. [1981] to produce a vertical ECO_2 distribution in the absence of a marine biosphere. See Figure 1a and the appendix for the model description. In the absence of the soft-tissue and carbonate pumps, the solubility pump alone determines the ECO_2 profile, unlike the real ocean, which is an as yet undetermined mixture of the three. Without biology, the model's solution reduces to a particularly simple form, with the profile determined by ECO_{2w} (the warm mixed layer concentration), ECO_{2u} (the concentration of the upwelling water at the base of the one-dimensional column), and a depth parameter, $z^* = K/w$, where K is the average vertical eddy diffusivity and w the upwelling velocity. Setting $z^* = 500$ m, calibrated from the globally-averaged vertical temperature profile [Hoffert et al., 1980], and requiring the inventory of CO_2 in the ocean-atmosphere system to be the same as measured by the Geochemical Ocean Sections Study (GEOSECS) of 3.16×10^{18} moles of CO_2 for the ocean [Takahashi et al., 1981a] reduces the problem to specifying a relationship between ECO_{2u} and ECO_{2w} . Their relation can develop a measure of the efficiency of the solubility pump.

As the overturning water moves from the warm surface box to the cold surface box, its pCO_2 will drop due to cooling, putting it below pCO_{2atm} and,

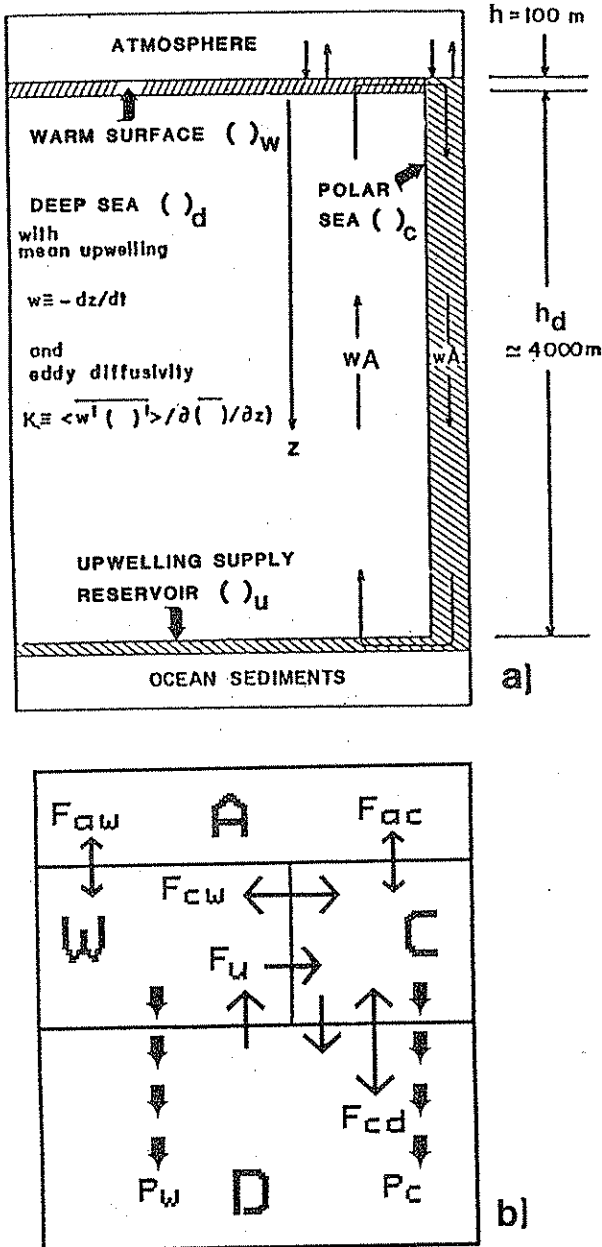


Fig. 1. (a) Schematic of the upwelling-diffusion model of Hoffert et al. [1980; 1981]. (b) Schematic of the Siegenthaler and Wenk [1984] model. Also see Wenk and Siegenthaler [this volume].

depending upon its residence time, will gain CO₂ from the atmosphere through the cold air-sea interface, determining its concentration, ECO_{2c} = ECO_{2u}. Two end-cases are possible.

Case 1. Cold water sinks from the surface in equilibrium with the atmosphere, i.e., pCO_{2c} = pCO_{2atm}.

Case 2. Cold water sinks from the surface at the ECO₂ concentration of the warm surface, i.e., ECO_{2c}

= ECO_{2w}. In this case of isochemical cooling, no CO₂ is picked up from the atmosphere.

Since case 1 is the maximum possible difference between ECO_{2c} and ECO_{2w}, it will create the largest possible gradient in an abiotic ocean's vertical ECO₂ profile and can be considered the case in which the solubility pump is the strongest. In case 2 the solubility pump is the weakest. We therefore define a solubility pump efficiency, η_{solu}, as

$$\eta_{\text{solu}} = (\Delta C_{\text{solu}}) / (\Delta C_{\text{solu,max}}) \quad (1)$$

where ΔC_{solu} and ΔC_{solu,max} are the actual and maximum surface-to-deep ECO₂ differences, respectively, due to the solubility pump. ΔC_{solu,max} is calculated as the amount of ECO₂ added to ECO_{2w} if the ECO_{2w} water is cooled to the cold region's temperature and equilibrated with pCO_{2atm}. In case 1 above, η_{solu} = 1.0 and in case 2, η_{solu} = 0.

In one-dimensional abiotic model, if ECO_{2c,eq} represents the ECO_{2c} for case 1, η_{solu} = (ECO_{2c} - ECO_{2w}) / (ECO_{2c,eq} - ECO_{2w}). For any given η_{solu}, there is a unique steady-state ECO₂ distribution that satisfies the constraint of constant CO₂ in the atmosphere-ocean system and with gas exchange simplified so that pCO_{2w} = pCO_{2atm} (see appendix).

Figure 2a shows the abiotic ECO₂ profile when η_{solu} = 1 and η_{solu} = 0 against the GEOSECS globally averaged data. Two points are apparent. First, with the solubility pump at its maximum efficiency, the surface-to-deep ECO₂ difference is less than that of the actual ocean. This demonstrates that the solubility pump alone could not produce the present ocean's ECO₂ profile. Second, the solubility pump can maintain a ECO₂ profile that is similar to the ocean's in respect to its causing a definite depletion of the surface ECO₂ relative to its deep value, i.e., ECO_{2w} < ECO_{2d}, thus demonstrating the pumping effect.

Figure 2b shows pCO_{2atm} as a function of η_{solu} for 0 < η_{solu} < 1. The resulting pCO_{2atm} varies from 720 μatm to 460 μatm, respectively, again demonstrating the pumping power of the solubility pump from its absence, η_{solu} = 0, to its maximum strength, η_{solu} = 1. With the soft-tissue and carbonate pumps on, the model produces a pCO_{2atm} of 260 μatm [Volk, 1984], therefore, assuming that η_{solu} = 1 in the abiotic state, this model calculates the presence of the marine biosphere maintains pCO_{2atm} 200 μatm lower than it would be otherwise. Although one could define the ΔpCO_{2atm} from pump minimum to pump maximum as a measure of strength, it will be more fruitful to define the pump's strength in terms of the surface-to-deep ECO₂ difference it creates, as discussed below, and which is different than the efficiency.

Note that the concept is unchanged if the ocean model has deep water upwelling into the polar sea, instead of being transported from the warm surface box. Typically, models such as Siegenthaler and Wenk's (1984) consider the polar surface as a mixture of transport between warm surface and cold surface and between deep and cold surface regions.

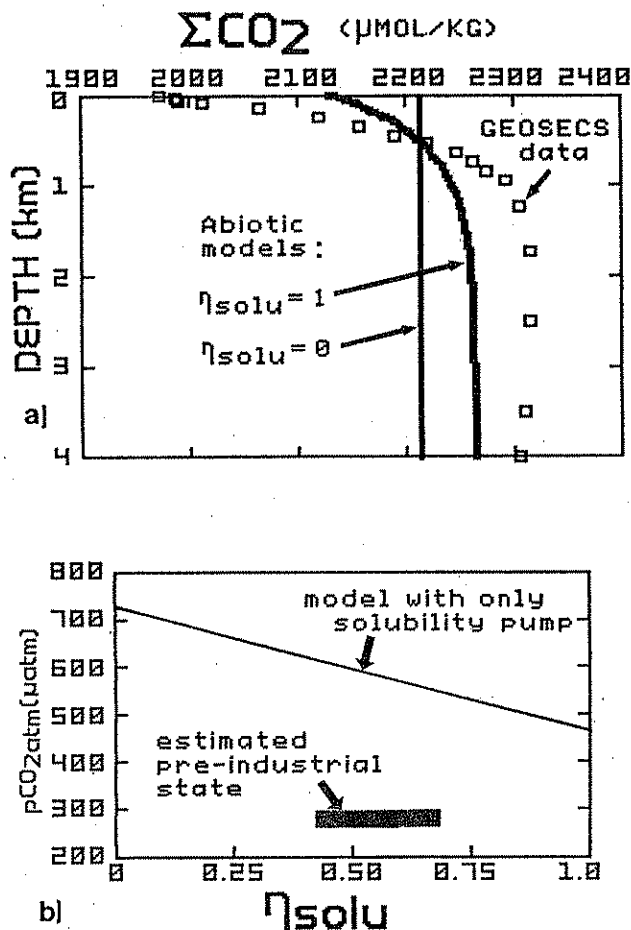


Fig. 2. (a) ECO_2 model profile of an abiotic ocean using the upwelling-diffusion model for a full and absent solubility pump, $\eta_{\text{solu}} = 1$ and $\eta_{\text{solu}} = 0$, respectively. The CO_2 in the model ocean-atmosphere system is a constant; the salinity-normalized GEOSECS data is from Takahashi et al. [1981b]. (b) Plot of $p\text{CO}_{2\text{atm}}$ as a function of the solubility pump's efficiency, η_{solu} , in an abiotic model. The η_{solu} for the preindustrial state is taken from Table 2.

The upwelling into the cold region from deep in an abiotic ocean could still be considered as between two extremes, reaching equilibrium with the atmosphere ($\eta_{\text{solu}} = 1$), or alternatively, upwelling under sea ice and having no gas exchange with the atmosphere ($\eta_{\text{solu}} = 0$).

Understanding the solubility pump by itself is relatively straightforward, but the real ocean and often models are a mixture of the three pumps. In order to begin a comparison, we first develop an efficiency for the soft tissue pump, similarly as was done for the solubility pump.

A soft-tissue efficiency, η_{soft} , is obtained by assuming that it is tied to the ocean's nutrient (PO_4 or NO_3) content. Then

$$\eta_{\text{soft}} = 1 - \text{PO}_{4\text{m}}/\text{PO}_{4\text{d}} \quad (2a)$$

$$\text{or} \quad \eta_{\text{soft}} = 1 - \text{NO}_{3\text{m}}/\text{NO}_{3\text{d}} \quad (2b)$$

with m representing the globally-averaged surface (mixed layer) concentration and d the globally-averaged deep concentration, with the depth interval defining d being the choice of the analyst. This formalizes two extremes in pump strength. If all nutrient available to the world ocean's surface is utilized for organic incorporation, $\text{PO}_{4\text{m}}$ or $\text{NO}_{3\text{m}} = 0$ $\eta_{\text{soft}} = 1$. If there is no biological utilization of available nutrient, $\text{PO}_{4\text{m}} = \text{PO}_{4\text{d}}$ or $\text{NO}_{3\text{m}} = \text{NO}_{3\text{d}}$ and $\eta_{\text{soft}} = 0$.

With η_{solu} and η_{soft} , we have a means to compare each pump to its own potential maximum. The efficiencies are not useful, however, in comparing the soft-tissue and solubility pump to each other. To assess the relative strengths of these two pumps in an ocean-atmosphere CO_2 system, we require a different type of measure, termed the pumping strength. This is accomplished by considering the surface-to-deep difference in ECO_2 each pump can create, independently of the other. Call these pumping strengths $\Delta\text{C}_{\text{solu}}$ and $\Delta\text{C}_{\text{soft}}$.

The soft-tissue strength, $\Delta\text{C}_{\text{soft}}$ can be straightforwardly measured in any model or ocean if the $[\text{C:P}]_{\text{soft}}$ Redfield ratio for organic matter is known and constant. Then,

$$\Delta\text{C}_{\text{soft}} = [\text{C:P}]_{\text{soft}} (\text{PO}_{4\text{d}} - \text{PO}_{4\text{m}}) \quad (3)$$

In any system that has only the solubility pump and the soft-tissue pump, $\Delta\text{C}_{\text{solu}}$ can then be calculated as

$$\Delta\text{C}_{\text{solu}} = (\text{ECO}_{2\text{d}} - \text{ECO}_{2\text{m}}) - \Delta\text{C}_{\text{soft}} \quad (4)$$

However, the problem is further complicated in that the real ocean and many models possess all three pumps combined in the ECO_2 signal. A means to disaggregate the carbonate pump signal from the ECO_2 data is a procedure fairly standard in chemical oceanography (Chen, 1978; Brewer, 1978) but for present purposes is most conveniently expressed by Fiadeiro (1980) who coined a tracer, C_{ox} , as the residual left from subtracting away the CaCO_3 contribution to the ECO_2 profile. Our modification of Fiadeiro's definition is

$$\text{C}_{\text{ox}} = \text{ECO}_2 - (1/2)(\text{TA} - \text{TA}_m + \text{NO}_3 - \text{NO}_{3\text{m}} + \text{PO}_4 - \text{PO}_{4\text{m}}) \quad (5)$$

We have modified Fiadeiro's original formulation by adding the constants TA_m , $\text{NO}_{3\text{m}}$, and $\text{PO}_{4\text{m}}$ so that $\text{C}_{\text{ox},\text{m}} = \text{ECO}_{2\text{m}}$, for interpretive convenience. Equation (5) assumes that 1 equivalent of TA is lost for every mole of NO_3 or PO_4 created. Although the ocean's PO_4 variation is within the range of uncertainty of the NO_3 measurements and essentially can be ignored in analyzing ocean data (Fiadeiro, 1980), in a model the TA change due to PO_4 as well as NO_3 can be exactly specified.

Equation (5) eliminates the carbonate pump

signal from ECO_2 data and therefore leaves only the solubility and soft-tissue pumps in the generated tracer of C_{ox} . Then we define a ΔC_{ox} , such that

$$\Delta C_{ox} = C_{ox,d} - C_{ox,m} \quad (6)$$

ΔC_{ox} must contain both remaining pump signals, so $\Delta C_{ox} = \Delta C_{soft} + \Delta C_{solu}$

$$\text{or } \Delta C_{solu} = \Delta C_{ox} - \Delta C_{soft} \quad (7)$$

Thus in any system consisting of all three pumps, the working strengths of the solubility and soft-tissue pump can be found knowing ECO_2 , TA, NO_3 , PO_4 , and $[C:P]_{soft}$ (or $[C:N]_{soft}$).

With the resulting n_{solu} , n_{soft} , ΔC_{soft} , and ΔC_{solu} we have information about the solubility and soft-tissue pumps' efficiencies (η 's) and strengths (AC's). The efficiencies are useful for comparing each pump to its own maximum and the strengths for comparing the pumps to each other. The next step is to use these formulations in analysis.

Analysis of Models

With the technique of pump strength analysis we make the following suggestions. Since the combined pump strengths were defined in terms of the surface-to-deep ECO_2 difference, any changes in a closed atmosphere-ocean carbon system that involves change in this difference should be a change in one or more of the pumps. The magnitude of change for each pump should be calculable. Second, since this kind of analysis has not been performed on models before, its use should give insight into the operation of models, both between different experiments with a particular model and between different models. The possibility for intermodel comparison is potentially most important, since up to this point the community has only had the rise or fall of pCO_{2atm} as a common effect to use in model comparison. The pumps should allow distinctions of similarities and differences regarding the causal connection between pCO_{2atm} and the processes within the models.

The first model to examine is that of Broecker and Takahashi (1984). There is a warm surface box and a cold deep box which outcrops in a polar sea. Thus both warm and deep boxes have contact with the atmosphere. A soft tissue pump is present only in the warm box; the alkalinity is constant, there is neither a carbonate pump nor TA changes associated with the soft-tissue pump.

Two ends states are calculated. In the first, the so-called Redfield-ocean, the warm-to-deep ECO_2 difference is fully determined by the particulate flux associated with the phosphate difference. Since $\Delta C_{solu} = 0$, by equation (1) $n_{solu} = 0$. This is an ocean with a soft-tissue pump only.

The other end state is the thermodynamic-ocean. Here an infinitely fast gas exchange brings both deep and warm boxes into equilibrium: $pCO_{2w} =$

$pCO_{2d} = pCO_{2atm}$. Now ΔC_{ox} is less than ΔC_{soft} . The ΔC_{soft} has remained identical to that of the Redfield-ocean because the PO_4 distribution is unchanged. From equation (7), this means ΔC_{solu} is less than 0. The solubility pump is only positive when the cold region is a sink for the atmospheric CO_2 flow. In this thermodynamic ocean, the cold region is a source. The rapid gas exchange reduces the ΔC_{ox} from the Redfield-ocean to that of $\Delta C_{solu,max}$. The soft-tissue pump remained constant in the two cases, while the solubility pump changed from 0 to a negative value between the Redfield- and thermodynamic-oceans. Accordingly, pCO_{2atm} increased in this change. A decrease in the sum of the strengths of the soft-tissue and solubility pumps increases pCO_{2atm} .

This shows we can understand the operation of the Broecker and Takahashi model through the carbon pumps. Furthermore, the absence of a positive solubility pump in their model suggests that the Redfield-ocean is not a true end state in the creation of the largest ΔC_{ox} possible. The maximum ΔC_{ox} in this model occurs when the $ECO_{2d} - ECO_{2w}$ is obtained solely from the soft-tissue pump. Can a positive solubility pump exist in addition to a soft tissue pump? A simple thought-experiment shows this to indeed be possible.

Consider an ocean with a warm surface box that shuttles water to a cold polar box. There it picks up CO_2 from the atmosphere; it then descends into a deep box and there receives the oxidation products from the soft-tissue pump. Therefore, its ΔC_{ox} is greater than ΔC_{soft} . This addition of a cold polar box with some exchange from a warm surface box is exactly the structure of the so-called high-latitude models of Siegenthaler and Wenk (1984), Knox and McElroy (1984), and Sarmiento and Toggweiler (1984).

These high-latitude models consist of three ocean boxes, a warm surface, a cold surface, and a deep box. Soft-tissue and carbonate pumps exist in both surface boxes, and various vertical and horizontal advective and exchange fluxes exist between the boxes. The Wenk and Siegenthaler (1985, this volume) model finds that decreased vertical exchange between the cold and deep boxes, increased horizontal exchange between the warm and cold boxes, and an increased biological flux from the cold box all individually reduce pCO_{2atm} . The causes for these pCO_{2atm} changes are not immediately comprehensible, and if the carbon pumps analysis is useful, then it should be able to elucidate new information from the high-latitude models.

We have constructed the Siegenthaler and Wenk model and run their standard-case and two circulation-change cases. See Figure 1b and the appendix for the model description. The soft-tissue pump's contribution to TA changes was treated more explicitly than in the Siegenthaler and Wenk documentation of the model so that equations (1), (2), (3), and (7) could be used to construct the efficiencies and strengths for the solubility and soft-tissue pumps for each model run.

TABLE 1. Three Box Model Analysis

Property	Box ^a	Standard Case (st)	1/2xF _{cd,st}	2xF _{ow,st}	Notes
pCO _{2atm} ^b	a	283	230	256	
PO ₄ ^c	w	0.30	0.30	0.30	
	c	1.43	1.06	1.23	
	m	0.42	0.38	0.40	
	d	2.24	2.24	2.24	
TA ^c	w	2324	2324	2324	
	c	2364	2351	2357	
	m	2329	2327	2328	
	d	2392	2392	2392	
CO ₂ ^c	w	1958	1913	1937	
	c	2158	2101	2127	
	m	1980	1934	1958	
	d	2284	2286	2285	
C _{ox} ^c	m	1980	1934	1958	Equation (5)
	d	2236	2238	2237	
ΔC _{ox} ^c		256	304	279	C _{ox,d} - C _{ox,m}
ΔC _{solu,max} ^c		170	178	173	Note d
ΔC _{soft} ^c		236	242	239	Equation (3)
η _{soft}		0.81	0.83	0.82	Equation (2)
ΔC _{solu} ^c		20	62	40	Equation (7)
η _{solu}		0.12	0.35	0.23	Equation (1)

Output of the Siegenthaler and Wenk [1984] model of Figure 1b, analyzed in terms of carbon pumps for each case.

a a,w,c and d refer to the atmosphere, warm surface, cold surface, and deep reservoirs of Figure 1b. m is the area-weighted average surface concentration; for this model $()_m = 0.89 ()_w + 0.11 ()_c$

b μatm

c μmol/kg

d C_{solu,max} is the amount of CO₂ that would be gained by C_{ox,m} if its pCO₂ equaled pCO_{2atm} at the polar temperature (3°C in this model), keeping TA_m and PO_{4m} constant.

Results are displayed in Table 1. It reveals that both the case of halving the cold-deep vertical exchange and that of doubling the warm-cold horizontal exchange reduce pCO_{2atm} primarily by increasing the solubility pump over the standard case. Take the first case. The ΔC_{soft} does increase slightly, from 236 μmol/kg to 242 μmol/kg, representing a change in η_{soft} from 0.81 to 0.83. However, the ΔC_{solu} increase is more substantial, from 20 μmol/kg to 62 μmol/kg, with the corresponding increase in η_{solu} from 0.12 to 0.35. The change in ΔC_{solu} is 7 times the change in ΔC_{soft}, showing that the pulling of additional CO₂ into the ocean in the lowering of pCO_{2atm} case is due to an

increase in strength of solubility pump. The case of doubling the warm-cold flux reveals the same underlying cause for the pCO_{2atm} change, an increase in solubility pump.

Knox and McElroy focused on changes in the marine biosphere in the cold box. By allowing the simulated glacial state's cold box PO₄ and NO₃ to go to zero from an interglacial state where PO₄ = 1.1 μmol/kg and NO₃ = 17 μmol/kg in the cold box, the model reduced pCO_{2atm} from 288 μatm to 161 μatm. It might superficially appear that this change was due to an increased soft-tissue pump. However, our carbon pump analysis of the model calculated that the ΔC_{soft} only slightly increased

from an interglacial 225 $\mu\text{mol/kg}$ to a glacial 231 $\mu\text{mol/kg}$ while ΔC_{solu} went from 22 $\mu\text{mol/kg}$ to 149 $\mu\text{mol/kg}$. It is actually the solubility pump, brought into full action in their glacial case, that caused the dramatic $p\text{CO}_{2\text{atm}}$ reduction. Although the soft-tissue pump in the cold box became stronger in the glacial state, it could do no more than contribute to reducing the entire model's surface nutrients to zero. For example, with a $\text{NO}_{3\text{d}} = 33 \mu\text{mol/kg}$ and a $[\text{C:N}]_{\text{soft}} = 7$, their soft-tissue pump acting at full strength, i.e., $\eta_{\text{soft}} = 1$, could contribute only 231 $\mu\text{mol/kg}$ to a ΔC_{ox} . The actual ΔC_{ox} in this case was 380 $\mu\text{mol/kg}$, a surface-to-deep C_{ox} (or ECO_2) difference impossible to achieve with the soft-tissue pump changes alone.

The result is that two circulation changes and one biological change of the high-latitude models are acting in a similar manner in that they each cause an increase in the solubility pump. This means that the carbon pumps analysis allows a level of understanding to be brought to bear on a model's specific causes and the $p\text{CO}_{2\text{atm}}$ results. Without a comparison of the strengths of the pumps, it is difficult to relate $p\text{CO}_{2\text{atm}}$ changes to their underlying causes. With such a comparison, numerous specific experiments may be related directly to changes they create in the carbon pumps.

Before moving on to an analysis of the GEOSECS ocean data, we note that in both interglacial cases of Siegenthaler and Wenk and Knox and McElroy, the ΔC_{ox} is greater than ΔC_{soft} , demonstrating the presence of a positive solubility pump that added to the ECO_2 difference made by the soft-tissue pump (and carbonate pump). Thus the Redfield-ocean of Broecker and Takahashi is an end state only in that particular model, not an end state for other models or for the ocean itself. One last point is that our doubling the $\text{CaCO}_3:\text{C}_{\text{soft}}$ ratio in the particulate flux from 0.2 (the standard case) to 0.4, a 100% increase in the carbonate pump, raised $p\text{CO}_{2\text{atm}}$ from 283 μatm to 309 μatm . This is relatively small compared to a typical reduction of 70 μatm in $p\text{CO}_{2\text{atm}}$ with an approximately 50% increase in the soft-tissue pump (Broecker, 1981).

Analysis of the Present Ocean State

What is the state of the carbon pumps in the ocean today; and can we deduce the former steady-state of the pre-industrial atmosphere-ocean system?

The GEOSECS data from Takahashi et al (1981b) for PO_4 , NO_3 , TA, and ECO_2 for ten ocean regions were area-weighted with data from Levitus (1982) to construct global surface (< 75 m) and deep (> 2000 m) water values. These are listed in Table 2 for four cases, the global values, the global values excluding the Antarctic Circumpolar area south of 50°S, the global values normalized to $S = 35\text{‰}$, and the global values excluding the Antarctic Circumpolar and normalized to $S = 35\text{‰}$. These four will show the differences that

arise in the analysis between including or excluding the Antarctic Circumpolar with its unusual surface properties and between the actual and salinity-normalized cases.

From the PO_4 , NO_3 , TA, and ECO_2 data, C_{ox} was constructed using equation (5). The problem that now arises is that the $C_{\text{ox,m}}$ ($\text{ECO}_{2\text{m}}$) measured during the GEOSECS was already somewhat increased over the preindustrial value by absorption of CO_2 from the $p\text{CO}_{2\text{atm}}$ transient driven by fossil fuel burning. The $p\text{CO}_{2\text{atm}}$ during GEOSECS was approximately 320 μatm , about 8 μatm above the globally-averaged $p\text{CO}_{2\text{atm}}$ of 312 μatm (Takahashi, personal communication, 1984). In a preindustrial steady-state, $p\text{CO}_{2\text{m}} = p\text{CO}_{2\text{atm}}$. The preindustrial $p\text{CO}_{2\text{atm}}$ is not known to perhaps less than 20 μatm . Moor and Stauffer (1984) indicate at preindustrial range of 270-280 μatm , while previous estimates gave a value closer to 260 μatm (Oeschger and Stauffer, 1984). We used the values of $\text{PO}_{4\text{m}}$, TA_{m} , $\text{ECO}_{2\text{m}}$ along with $S = 35\text{‰}$ and $\text{SI} = 5 \mu\text{mol/kg}$ and adjusted the T_{m} for each of the four cases until a $p\text{CO}_{2\text{m}} = 312 \mu\text{atm}$ was returned from the equilibrium carbonate chemistry (see appendix). The $p\text{CO}_{2\text{m}}$ was then changed to $270 \pm 10 \mu\text{atm}$ for the four cases. The $\text{ECO}_{2\text{m}}$ differences between the $p\text{CO}_{2\text{m}} = 312 \mu\text{atm}$ and $p\text{CO}_{2\text{atm}} = 270 \mu\text{atm}$ varied by less than 3% in the four cases. The correction to $C_{\text{ox,m}}$ for a preindustrial $p\text{CO}_{2\text{atm}} = 270 \pm 10 \mu\text{atm}$ was determined to be $-31 \pm 9 \mu\text{mol/kg}$. This correction is applied to obtain a preindustrial $C_{\text{ox,m}}$ in Table 2.

Another assumption in this analysis is that of $[\text{C:P}]_{\text{soft}} = 105$, as in Redfield et al (1963). Recent work by Takahashi et al (1985) using isopycnal surfaces indicates $[\text{C:P}]_{\text{soft}} = 103$ if C_{ox} and PO_4 are examined directly, but $[\text{C:P}]_{\text{soft}} = 140$ if O_2 and NO_3 are used to deconvolve the C_{ox} variation. Table 2 shows the ΔC_{soft} using equation (3) and $[\text{C:P}]_{\text{soft}} = 105$.

Using the preindustrial $C_{\text{ox,m}}$ and the GEOSECS $C_{\text{ox,d}}$, ΔC_{ox} is obtained and is significantly larger than ΔC_{soft} . This indicates the presence of a positive solubility pump signal in the globally-averaged ocean. The ΔC_{solu} is obtained using equation (7).

Equation (2) calculates η_{soft} , which is higher in the cases that excluded the Antarctic circumpolar area ($\eta_{\text{soft}} = 0.85$) than in the global value ($\eta_{\text{soft}} = 0.77$), because the high nutrient values in the circumpolar represent an inefficiency in the soft-tissue pump.

To obtain an ocean value of $\Delta C_{\text{solu,max}}$, water with properties of $\text{PO}_{4\text{m}}$, TA_{m} , $\text{SA} = 35\text{‰}$, $\text{SI} = 5 \mu\text{mol/kg}$, and $T = 1.5^\circ\text{C}$ was equilibrated with $p\text{CO}_{2\text{atm}} = 312 \mu\text{atm}$ using the carbonate chemistry routines to calculate a maximum C_{ox} that could be created by the solubility pump alone. The difference between this value and $C_{\text{ox,m}}$ (GEOSECS) gives a $\Delta C_{\text{solu,max}}$ and finally η_{solu} from equation (1). The range of η_{solu} for the four cases for the $p\text{CO}_{2\text{atm}}$ pre-industrial value of $270 \pm 10 \mu\text{atm}$ is 0.43 - 0.68. Efficiency values for the S-normalized cases were about 0.06 higher than the non-normalized cases and the cases omitting the

TABLE 2. GEOSECS Data Analysis^a

Property ^b	Depth (m)	Global	Global without Antarctic Circumpolar Area	Global S=35 /oo	Global without Antarctic Circumpolar Area, S = 35 ^o /oo	Notes
PO ₄	<75	0.50	0.33	0.51	0.33	
	>2000	2.20	2.20	2.21	2.22	
NO ₃	<75	5.48	2.60	5.62	2.59	
	>2000	32.60	32.66	32.87	32.93	
TA	<75	2324	2327	2322	2314	
	>2000	2395	2400	2414	2419	
TCO ₂	<75	2016	1997	2016	1985	
	>2000	2288	2292	2306	2310	
C _{ox}	<75	2016	1997	2016	1985	Equation (5)
	>2000	2238	2240	2246	2242	
C _{ox}	<75	1985 ± 9	1966 ± 9	1985 ± 9	1954 ± 9	Preindustrial (see text)
	>2000	2238	2240	2246	2242	
ΔC _{ox}		253 ± 9	274 ± 9	260 ± 9	288 ± 9	Preindustrial (C _{ox,d} -C _{ox,m})
ΔC _{solu,max}		136	159	135	159	See text
ΔC _{soft}		178	196	178	198	Equation (3)
η _{soft}		0.77	0.85	0.77	0.85	Equation (2)
ΔC _{solu}		74 ± 9	78 ± 9	82 ± 9	90 ± 9	Equation (7) Preindustrial
η _{solu}		0.54 ± 0.07	0.49 ± 0.06	0.61 ± 0.07	0.56 ± 0.06	Equation (1)

^a Global data from GEOSECS [Takahashi et al. 1981b] used to calculate the global properties of the soft-tissue and solubility pumps, using area-weighting from Levitus [1982].

^b μmol/kg, except for the non-dimensional η_{solu} and η_{soft}.

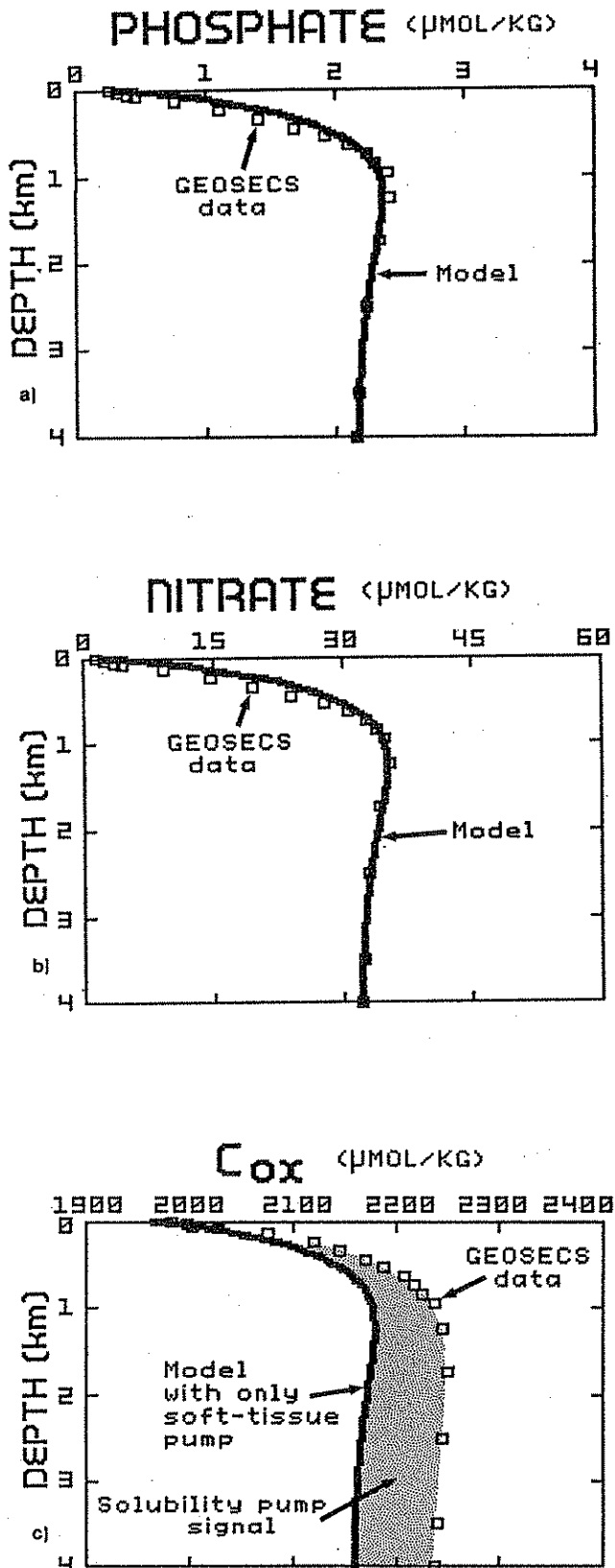
Antarctic circumpolar about were 0.05 lower than the global cases.

According to this analysis, there is a solubility pump operating in the ocean's ECO₂ signal at about 50% efficiency. It creates a global ECO₂ surface-to-deep difference (ΔC_{solu}) of 74 μmol/kg for the global, non-S-normalized case, compared to the difference created by the soft-tissue pump (ΔC_{soft}) of 178 μmol/kg. The solubility pump's strength appears therefore to be about 40% that of the soft tissue pump.

This analysis is subject to uncertainty in the preindustrial pCO_{2atm} and in the [C:P]_{soft} ratio. For example, the solubility pump signal disappears

from the analysis if [C:P]_{soft} = 140 and if pCO_{2atm} was somewhat above 280 μatm. More certain analysis of the ocean data with the technique of pump strengths would have to wait for more accuracy in these values.

Finally, the 1-D upwelling-diffusion model is used with an internal source term to simulate a global PO₄ profile in Figure 3a. See the appendix for details. Using the PO₄ model as a calibration, fluxes associated with the internal source term and the change of warm surface water into bottom upwelling water are scaled by N:P = 16:1, and a NO₃ model is produced in Figure 3b. This scaling of fluxes then is put at 105:1 to create a C_{ox}



profile with $C_{\text{Ox},m}$ (preindustrial) = 1966 $\mu\text{mol/kg}$. This C_{Ox} model profile does not match the actual C_{Ox} profile, generated from the GEOSCECS data. The difference between the data and the model is the visual representation of the presence of the solubility pump as quantified in Table 2.

Discussion

A technique for analyzing a three-component carbon pump system has been developed. Treatment of the carbonate pump was primarily to subtract it from the data to show a combined signal of the solubility and soft-tissue pumps. These can be isolated through nutrient-carbon coupling.

The technique has proven useful in a variety of instances. The Broecker and Takahashi [1984] ocean circulation change study apparently centers around the variation of the solubility pump between zero and a negative value. That the solubility pump can be negative has to do with what will now be shown to be a relationship between the soft-tissue and solubility pumps.

With the present ocean PO_4 average content of about 2 $\mu\text{mol/kg}$, if $n_{\text{soft}} = 1$ a maximum ΔC_{soft} can be maintained that is $105 \times 2 = 210 \mu\text{mol/kg}$. For today's values of ECO_{2m} , T_m , and S , the difference in equilibrium ECO_2 between 20°C and 2°C at a constant and approximately current $p\text{CO}_{2\text{atm}}$ is a $\Delta C_{\text{solu,max}}$ of about 140-170 $\mu\text{mol/kg}$. That the present $\Delta C_{\text{soft,max}}$ is larger than $\Delta C_{\text{solu,max}}$ is important because it means that if deep water such that $(\text{ECO}_{2d} - \text{ECO}_{2m}) > \Delta C_{\text{solu,max}}$ upwells in the polar regions, its $p\text{CO}_2$ will be greater than $p\text{CO}_{2\text{atm}}$, and the region will outgas CO_2 to the atmosphere and be a source. In this case the ocean would not be able to take advantage of the solubility pump. On the other hand, if the average PO_4 content was only 1 $\mu\text{mol/kg}$, then the polar regions could only be sinks.

Our analysis indicates that the three-box high-latitude models exhibit variations primarily in their solubility pump. How does this work? One example is the case of decreased exchange between

Fig. 3. (a) Model-generated PO_4 profile using the upwelling-diffusion model with a calibrated internal source term ($J(z)$) and a parameterization (F_{WU}) of preformed PO_4 and entrained PO_4 . (b) Model-generated NO_3 scaling the $J(z)$ and F_{WU} from the PO_4 model by $\text{N:P} = 16:1$. (c) Model-generated C_{Ox} profile scaling $J(z)$ and F_{WU} to PO_4 by $[\text{C:P}]_{\text{soft}} = 105$. This profile, like that of PO_4 and NO_3 , contains only a soft-tissue pump, while the C_{Ox} data will have both solubility and soft-tissue pumps (the carbonate pump was eliminated in forming C_{Ox} , see equation (5)). The possible presence of a positive solubility pump in the data is shown by the gap between model and data. $C_{\text{Ox},w}$ was taken as 1966 $\mu\text{mol/kg}$, for a preindustrial $p\text{CO}_{2\text{atm}}$ of 270 μatm (see Table 2). The GEOSCECS data is for in situ salinity from Takahashi et al. [1981b].

the deep and cold surface boxes. The deep box can be thought of as contaminating the cold box's possibility to use the solubility pump, since exchange with the deep box brings water into the cold box such that $(C_{ox,d} - C_{ox,m}) > \Delta C_{solu,max}$ and its presence will therefore reduce the effectiveness of the solubility pump. It appears that a slight inefficiency in the global biological pump, if it occurs in the polar regions, can clog the solubility pump. This is a linkage between the two. This clogging of the solubility pump is due to its dependence on a small region of the world's ocean surface for operation, while the soft-tissue pump acts vertically everywhere. The solubility pump's downward vertical action of water potentially enriched in ΔC_{solu} occurs only in the polar regions in these models. In the ocean, intermediate waters also may act as parts of the solubility pump. This should be examined.

These demonstrations of the pump analysis have been with the simplest models. Further tests of the technique should apply the analysis to more detailed models, such as the twelve-box global model of Bolin et al. [1983] and the two-dimensional model of Baes and Killough [1985]. Do solubility pump signals exist in the steady-states of these models? Can the analysis, which depends here upon a global aggregation of concentrations, be useful in more complex models?

Hopefully, yes, for the technique appears to be of use in looking at the aggregated GEOSECS data. If any model's ΔC_{ox} is greater than ΔC_{soft} then the solubility pump is present. It should not matter how many horizontal boxes have to be averaged to obtain the aggregated data for the pump analysis. In some ways, the models are more attractive domains for the application of the technique than the actual ocean, because the Redfield ratios in models are specified exactly, unlike the situation in the ocean.

The main accomplishment has been to add a level in the causal hierarchy. Specific ocean changes can cause changes in the pumps which affect pCO_{2atm} . This should facilitate a classification of model types. Perhaps all ocean-driven CO_2 changes can be put into the pump scheme. For example, the phosphate extraction model [Broecker, 1981] is clearly a variation of the soft tissue pump. Furthermore, new questions can be asked. For instance, does an increased soft-tissue pump due to elevated PO_4 levels aid in clogging the polar regions and therefore decrease the solubility pump? Distinguishing the strengths and efficiencies of the pumps may help formulate questions about models and possible ocean changes in the future.

Appendix: Model Calculations

Routines to calculate pCO_2 from ECO_2 or ECO_2 from pCO_2 , knowing TA, T, S, PO_4 , and SI were provided to us by T. Takahashi. The calculations essentially follow those presented by Takahashi et al. [1982].

The three-box ocean model in Figure 1b and results in Table 1 are from Siegenthaler and Wenk [1984]. In our calculations, each mole of NO_3 and PO_4 created is taken to decrease TA by 1 equivalent. The $CaCO_3:C_{soft}$ ratio is 0.2, making the $PO_4:NO_3:TA:ECO_2$ ratio in the particulate fluxes 1:16:35:156. The standard case values of average levels of PO_4 , TA, and ECO_2 and the fluxes and conditions for solution are given in Siegenthaler and Wenk [1984] and Wenk and Siegenthaler [this volume].

For the one-dimensional upwelling-diffusion model of Figure 1a, the physical parameters are a vertical eddy diffusivity (K) in square meters per year, and an upwelling velocity (w) in meters per year. A soft-tissue biological source term (J) in moles per cubic meter year is assumed to decrease exponentially with depth according to

$$J(z) = J_0 \exp(-z/z_{ox})$$

where J_0 is the soft-tissue pump source at $z = 0$ and z_{ox} is a depth parameter for the soft-tissue pump. Designating F_g as the total flux of soft-tissue leaving the mixed layer to be oxidized in the water column during a year's time,

$$F_g = J_0 \int_0^{h_d} \exp(-z/z_{ox}) dz \quad (8a)$$

Then J_0 can be expressed in terms of F_g specifically for oxidation

$$J_0 = F_g / [z_{ox}(1 - \exp(-h_d/z_{ox}))] \quad (8b)$$

The general one-dimensional tracer equation for any property C is then written as

$$dC/dt = Kd^2C/dz^2 + wC/dz + J_0 \exp(-z/z_{ox}) \quad (9)$$

The steady state solution is

$$C(z) = B_1 + B_2 \exp(-zw/K) + B_3 \exp(-\frac{z}{z_{ox}}) \quad (10)$$

where $B_3 = F_g / [(1 - \exp(-h_d/z_{ox})) (w - K/z_{ox})]$ and B_1 and B_2 are to be solved for from two boundary conditions.

We can specify a mixed layer concentration as an upper boundary condition and a bottom flux balance as a lower boundary condition, as in the work by Hoffert et al. [1980]: (1) $C_0 = C_w$ (specified from data) and (2) $wC_u = wC_{hd} + K(dC_{hd}/dz)$ estimating from data the upwelling concentration, (C_u), of water entering the diffusive field. Then, $B_1 = C_u - B_3(1 - \exp(-z^*/z_{ox})) \exp(-h_d/z_{ox})$ and $B_2 = C_w - B_1 - B_3$ where $z^* = K/w$.

For the abiotic ocean (Figure 2), $F_g = B_3 = 0$, and the solution simplifies to

$$C(z) = C_u + (C_w - C_u) \exp(-z/z^*) \quad (11)$$

For the abiotic solution, the following properties were assumed to be well mixed, equal to their GEOSECS global averages normalized to $S = 35\text{‰}$ [Takahashi et al. 1981a, 1981b] and therefore the values for the warm and cold surface boxes: $TA = 2387 \mu\text{eq/kg}$, $S = 35\text{‰}$, $PO_4 = 2.1 \mu\text{mol/kg}$, $SI = 100 \mu\text{mol/kg}$. Also, $T_w = 20^\circ\text{C}$ and $T_c = 1.5^\circ\text{C}$. The area of the world ocean was $3.34 \times 10^{14} \text{m}^2$ and total ocean-atmosphere inventory of 3.22×10^{18} moles of CO_2 . The calculation at a specified n_{solu} begins by guessing ECO_{2w} , obtaining $p\text{CO}_{2w}$ by Takahashi et al. [1982] routines, setting $p\text{CO}_{2\text{atm}} = p\text{CO}_{2w}$ and obtaining $\text{ECO}_{2c} = \text{ECO}_{2u}$ from equation (1):

$$\text{ECO}_{2u} = \text{ECO}_{2w} + n_{\text{solu}}(\text{ECO}_{2c, \text{eq}} - \text{ECO}_{2w})$$

Using $K = 2000 \text{m}^2/\text{yr}$, $w = 4 \text{m}/\text{yr}$ and $z^* = 500 \text{m}$ [Hoffert et al. 1980], equation (11) produces the $\text{ECO}_2(z)$ profile. The amount of CO_2 in the atmosphere-ocean model is compared to the desired inventory. An iterative procedure follows by guessing a new ECO_{2w} until convergence to the inventory.

This calculation does not require specification of a cold surface area or gas exchange coefficient, although this could be done. The interest is on the solubility pump efficiency, so area and gas exchange rate could be adjusted to obtain any particular ECO_{2c} . Since $A_w < A_c$, generally in models and in the ocean, $p\text{CO}_{2w} = p\text{CO}_{2\text{atm}}$. With the cold surface as a sink, $p\text{CO}_{2w}$ would be several microatmospheres above $p\text{CO}_{2\text{atm}}$ for a steady state in the atmosphere. This error in obtaining Figure 2b is much less than the uncertainty in the other parameters.

For the one-dimensional upwelling-diffusion model with soft-tissue pump (Figure 3), we use equation (10). A fit to PO_4 GEOSECS data (Figure 3a) was obtained with $F_g = 4500 \mu\text{mol}/^2\text{yr}$ and $z_{\text{ox}} = 770 \text{m}$. PO_{4u} and PO_{4w} were set at $2.18 \mu\text{mol/kg}$ and $0.33 \mu\text{mol/kg}$, respectively. This mathematically implies a PO_4 flux (F_{wu}) between warm surface layer and bottom upwelling water of $F_{wu} = \rho w(PO_{4u} - PO_{4w}) = 7600 \mu\text{mol}/\text{m}^2\text{yr}$, where ρ is the density of seawater. The F_{wu} flux may physically represent preformed properties that upwell through the one-dimensional column directly into the cold surface and/or entrainment of properties by the downwelling plume of bottom water formation [see Southam and Peterson, this volume]. The point is that the PO_4 model is a calibration. The NO_3 and CO_x models are produced from the PO_4 model calibration by scaling the F_g and F_{wu} fluxes with Redfield ratios: $F_g, PO_4: F_g, \text{NO}_3: F_g, \text{CO}_x = F_{wu}, PO_4: F_{wu}, \text{NO}_3: F_{wu}, \text{CO}_x = 1:16:105$.

Note that this CO_x model contained the soft-tissue pump only. The NO_3 model scales quite well from PO_4 , but the CO_x with soft-tissue pump only does not make the surface-to-deep difference shown by the GEOSECS data of Figure 3c, implying the existence of a solubility pump if the Redfield ratios are correct.

Acknowledgements. This research was supported by the Department of Energy, Carbon Dioxide Research Division, Office of Basic Energy Sciences, under contract DE-AC02-81EV10610 to New York University. Many thanks to Taro Takahashi for numerous invaluable discussions and for supplying the chemical formulations determining the CO_2/ECO_2 system.

References

- Baes, C.F., Jr., and G.G. Killough, Chemical and biological processes in CO_2 -ocean models, Oak Ridge Natl. Lab. Life Sci. Symp. Global Carbon Cycle, 6th, in press, 1985
- Bolin, B.A. Bjorkstrom, K. Holmen, and B. Moore, The simultaneous use of tracers for ocean circulation studies, Tellus, 35B, 206-236, 1983.
- Brewer, P.G., Direct observation of the oceanic CO_2 increase, Geophys. Res. Lett., 5, 997-1000, 1978.
- Broecker, W.S., Glacial to interglacial changes in ocean and atmosphere chemistry, in Climatic Variations and Variability: Facts and Theories, edited by A. Berger, pp. 111-121 D. Reidel, Hingham, Mass., 1981.
- Broecker, W.S., The ocean, Sci. Am., 249, 146-161, 1983.
- Broecker, W.S., and T. Takahashi, Is there a tie between atmospheric CO_2 content and ocean circulation?, in Climate Processes and Climate Sensitivity, Geophys. Monogr. Serv., Vol. 29, edited by J.E. Hansen and T. Takahashi, pp. 314-326, AGU, Washington, D.C., 1984.
- Chen, C-T. A., Decomposition of calcium carbonate and organic carbon in the deep oceans, Science, 210, 735-736, 1978.
- Ennever, F.K., and M.B. McElroy, Changes in atmospheric CO_2 : Factors regulating the glacial to interglacial transition, this volume.
- Fladeiro, M.E., Carbon cycling in the ocean, in Primary productivity in the Sea, edited by P. Falkowski, pp. 487-496, Plenum, New York, 1980.
- Hoffert, M.I., A.J. Callegari, and C.T. Hsieh, The role of deep sea heat storage in the secular response to climatic forcing, J. Geophys. Res., 85, 6667-6679, 1980.
- Hoffert, M.I., A.J. Callegari, and C.T. Hsieh, A box-diffusion carbon cycle model with upwelling, polar bottom water formation and a marine biosphere, in Carbon Cycle Modeling: Scope 16, edited by B. Bolin pp. 287-305, John Wiley, New York, 1981.
- Keeling, C.D., and B. Bolin, The simultaneous use of chemical tracers in oceanic studies: A three-reservoir model of the North and South Pacific oceans, Tellus, 20, 17-54, 1968.
- Knox, F., and M.B. McElroy, Changes in atmospheric CO_2 : Influence of the marine biota at high latitude, J. Geophys. Res., 89, 4629-4637, 1984.
- Levitus, S., Climatological Atlas of the World Ocean, NOAA Prof. Pap. 13, U.S. Dept. of Commer., Washington, D.C., 1982.
- Maier-Reimer, E., A three-dimensional ocean carbon cycle model, paper presented at Chapman

- Conference on Natural Variations in Carbon Dioxide and the Carbon Cycle, AGU, Tarpon Springs, Fla., Jan. 9-13, 1984.
- Moor, E., and B. Stauffer, A new dry extraction system for gases in ice, J. Glaciol., in press, 1984.
- Neftel, A., H. Oeschger, J. Schwander, B. Stauffer, and R. Zumbunn, Ice core measurements give atmospheric CO₂ content during the last 40,000 years, Nature, 295, 220-223, 1982.
- Oeschger, H., and B. Stauffer, Review of the history of the atmospheric CO₂ recorded in ice cores, Oak Ridge Natl. Lab. Life Sci. Symp. Global Carbon Cycle, 6th. in press, 1985.
- Redfield, A.C., B.H. Ketchum, and F.A. Richards, The influence of organisms on the composition of sea-water, in The Sea, Vol.2, edited by M.N. Hill, pp. 26-77, Interscience, New York, 1963.
- Sarmiento, J.L., and J.R. Toggweiler, A new model for the role of the oceans in determining atmospheric pCO₂, Nature, 308, 620-624, 1984.
- Siegenthaler, U., and T. Wenk, Rapid atmospheric CO₂ variations and ocean circulation, Nature, 308, 624-626, 1984.
- Southam, J. R., and W. H. Peterson, Transient response of the marine carbon cycle, this volume.
- Takahashi, T., W. S. Broecker, and A.E. Bainbridge, The alkalinity and total carbon dioxide concentration in the world oceans, in Carbon Cycle Modeling; Scope 16, edited by B. Bolin, pp. 271-286, John Wiley, New York, 1981a.
- Takahashi, T., W.S. Broecker, and A. E. Bainbridge, Supplement to the alkalinity and total carbon dioxide concentration in the world oceans, in Carbon Cycle Modeling; Scope 16, edited by B. Bolin, pp. 159-200, John Wiley, New York, 1981b.
- Takahashi, T., R.T. Williams, and D.L. Bos, Carbonate chemistry, in GEOSECS Pacific Expedition, Vol. 3, Hydrographic Data, 1973-1974, Chap. 3, U.S. Government Printing Office, Washington, D.C., 1982.
- Takahashi, T., W.S. Broecker, and S. Langer, Redfield ratio based on chemical data from isopycnal surfaces, J. Geophys. Res., in press, 1985.
- Toggweiler, J.R., and J.L. Sarmiento, Glacial to interglacial changes in atmospheric carbon dioxide: The critical role of ocean surface waters in high latitudes, this volume.
- Volk, T., Multi-property modeling of the marine biosphere in relation to global climate and carbon cycles, Ph.D. thesis, 348 pp., New York Univ., New York, May 1984.
- Wenk, T., and U. Siegenthaler, The high-latitude ocean as a control of atmospheric CO₂, this volume.